Journal of Interdisciplinary Mathematics
ISSN: 0972-0502 (Print), ISSN: 2169-012X (Online)
Vol. 28 (2025), No. 7, pp. 2567–2600
DOI : 10.47974/JIM-2063

Optimal control analysis of malaria and typhoid fever co-dynamics

S. Y. Tchoumi *
Department of Mathematics and Computer Sciences
ENSAI, University of Ngaoundere
P. O. Box 455
Ngaoundere
Cameroon

and

Department of Mathematics and Applied Mathematics
University of Pretoria
Pretoria
South Africa

C. W. Chukwu †
Department of Mathematical Sciences
Georgia Southern University
65 Georgia Ave.
P.O. Box 8093, Statesboro
Georgia 30460
U.S.A.

M. L. Diagne §
Departement de Mathematiques
UFR des Sciences et Technologies
Universite de Thies
Thies
Senegal

H. Rwezaura ‡
Department of Mathematics
University of Dar es Salaam
P. O. Box 35062
Dar es Salaam
Tanzania

* *E-mail:* sytchoumi83@gmail.com (Corresponding Author)
† *E-mail:* wiliam.chukwu@gmail.com
§ *E-mail:* couragelamine@gmail.com
‡ *E-mail:* heriethrwezaula@gmail.com

© Taru Publications

J. M. Tchuenche [@]
School of Computer Science and Applied Mathematics
University of the Witwatersrand
Private Bag 3, Wits 2050
Johannesburg
South Africa

and

School of Computational and Communication Sciences and Engineering
Nelson Mandela African Institution of Science and Technology
P. O. Box 447
Arusha
Tanzania

Abstract

Malaria is an infectious vector-borne disease spread by infected mosquitoes, while typhoid fever is contracted by either drinking water or eating food contaminated with the Salmonella typhoid bacteria. Both diseases affect millions of individuals every year, causing a great deal of morbidity and mortality. Previous mathematical models of the co-dynamics of these two diseases have not considered the interplay between symptomatic and asymptomatic individuals infected with typhoid. To fill this gap, we formulate a malaria and typhoid co-infection model explicitly including both of these classes and use standard theory of dynamical systems to analyze the model. The sub-models reproduction numbers are derived. Theoretical results show that the disease-free and endemic equilibria could co-exist (backward bifurcation) for both the typhoid only and malaria only sub-models when the respective reproduction number is less than unity. The potential impact of malaria on typhoid reveals that the increase in the number of cases due to malaria could lead to a decrease of the number of typhoid fever cases. To mitigate the spread of both malaria and typhoid fever, the model is extended to include three control measures: malaria prevention, typhoid vaccination and treatment. Numerical simulations are carried out and graphically depicted, and it is noted that reduction in the spread of typhoid greatly impacts the decrease in the number of malaria infectious individuals. Also, as expected, the most effective combination control strategy is the simultaneous implementation of malaria prevention, typhoid treatment and vaccination.

Subject Classification (2020): *34D20, 34D23, 49K10, 49M05, 92B05, 92D30.*

Keywords: *Malaria, Typhoid fever, Co-infection, Optimal control, Mathematical model, Basic reproduction number.*

[@] *E-mail:* **jmtchuenche@gmail.com**

1. Introduction

Malaria, an infectious vector-borne disease is mainly transmitted by the Plasmodium falciparum parasite (which is the most dangerous strain) and spread by infected female Anopheles mosquito. Malaria usually presents symptoms such as chills, fever, general discomfort, headache, nausea and vomiting, diarrhea, abdominal pain, muscle or joint pain, fatigue, rapid breathing, and cough [1, 18]. From the 2021 World Malaria Report, in 2020, Malaria was estimated to have resulted in 241 million cases, 627,000 deaths, with the highest number of deaths (77%) in children less than 5 years old. Overall, 90% of Malaria cases and deaths were reported in Africa [33, 38].

Typhoid fever caused by Salmonella *typhi* is an acute illness associated with severe fever. Humans contract the disease by ingesting the bacteria in contaminated food or water. Infected individuals then contaminate the environment such as water reservoir or supply through stool. Typhoid infected individuals usually present symptoms as poor appetite, headache, fever as high as 104 degrees Fahrenheit, and sometimes diarrhea [2]. According to the World Health Organization (WHO), approximately 11 to 20 million people develop typhoid fever, with approximately 128,000 to 161,000 people dying from this disease annually [3]. Children 5 to 15 years old are generally at the highest risk of contracting the disease, and those under the age of 5 have the highest death risk in typhoid endemic countries [2].

Epidemiologically, co-dynamics refers to a simultaneous or dual infection of an indivual by two or more pathogens such as viruses, bacteria, or fungi [16, 27]. An association between malaria and typhoid fever was first described in the medical literature in the middle of the 19^{th} century and was named *typhomalarial fever* by the United States Army [13, 32]. Other studies confirmed the relationship/association as well as the geographical overlap between malaria and salmonellae by describing a higher incidence of non-typhoidal salmonella bacteremia among patients with malarial parasitemia [8, 12].

Several mathematical modeling studies consider either malaria only or typhoid fever only [4, 34, 35], to name a few, and the literature therein. Studies of the co-dynamics of both diseases are not new. Mushayabasa *et al.,* in [23] studied a malaria-typhoid co-dynamics model, which only considers the direct transmission of typhoid (person-to-person) and assumes no recovery of co-infected individuals from single disease. In [24], the authors noted that a typhoid outbreak in malaria endemic settings might lead to higher cumulative cases of dually-infected individuals displaying clinical symptoms common to both diseases. It has been noted that false diagnoses with higher possible cases for typhoid than malaria could cause a significant devastating impact on Kenyan societies, a reminder that both diseases must be managed simultaneously for successful control of co-epidemics [25]. Typhoid fever and malaria, as well as their co-infection, could persist in the community as it has been shown that the reproduction number of the co-dynamics of malaria and typhoid fever could be higher than unity [39]. Thus, to reduce the spread of both diseases, attention

should be paid to key sensitive parameters such as the transmission or contact rate of typhoid fever, the *per capita* mosquito biting rate [5, 24]. In [5], the classical Susceptible-Infected-Recovered (SIR)-type malaria and typhoid co-dynamics model incorporating vector and loss of immunity by humans is considered. Their results show that a high number of malaria and typhoid fever infected individuals increases the value of mosquito biting rate mainly because there are more idle infected individuals on which mosquitoes can feed. In general, the best strategy to minimize or eradicate malaria-typhoid co-dynamics in any population is to reduce the transmission probabilities of malaria (that is, mosquito biting rates) and typhoid, which in turn decreases the rate of the reproduction number below unity. Workie and koya [39] analyzed a deterministic model of typhoid fever with *Plasmodium Vivax* and *Plasmodium Falciparum* co-dynamics that incorporates treatment. Their results suggest that to eradicate the disease, one needs to implement (i) appropriate treatment, (ii) reduce the reproduction number by decreasing the contact rate with typhoid fever and malaria infectious individuals, and (iii) protect the human population from mosquitoes bites through the use of different malaria and typhoid fever control strategies. Analytical results from [24] showed that typhoid and malaria co-dynamics model could exhibit a backward bifurcation phenomenon. In contrast, numerical results in [7, 25, 31] suggest that a typhoid outbreak in malaria-endemic settings may lead to a higher population of co-infected individuals than the mono-infected population.

Only few of the studies cited above incorporate optimal control in their malaria and typhoid fever co-dynamic model and do not take into account the transitions between asymptomatic and symptomatic typhoid cases, which is a major challenge in the control of this disease. Herein, we propose a mathematical model of the co-dynamics of malaria and typhoid fever that integrates the transition from asymptomatic to symptomatic. This model is analyzed with and without optimal control, the latter referring to analyzing the model where decisions are made continuously over time, considering changing information. The optimal control section follows the same approach as in [36] where three control interventions denoted by c_1, c_2 and c_3 representing malaria prevention, typhoid fever vaccination and typhoid fever treatment, respectively are incorporated. We numerically evaluate various strategies, that is the outcome of combining different interventions related to each control on the fight against co-dynamic malaria and typhoid fever with the aim of finding the best strategy or combination of these controls that allows to better mitigate the spread of both diseases and their co-infection. As expected, implementation of the three control strategies is more effective to mitigate the spread of malaria and typhoid fever in a community [36].

In what follows, the proposed mathematical model of co-dynamics of malaria and typhoid fever is formulated in Section 2. Section 3 is the theoretical analysis of the model. Optimal control is carried out in Section 4, while Section 5 presents the numerical simulation (graphical representation). Section 6 is the conclusion.

2. Model formulation

During the course of typhoid fever, infected individuals pass through various epidemiological classes, as represented in Figure 1. In what follows, it is assumed that the asymptomatic infected with typhoid fever A_t cannot recover naturally, and that infectious individuals with individuals co-infected with malaria and typhoid fever should be treated simultaneously for both diseases, and after recovery, they become susceptible again and move into the susceptible compartment.

We consider three types of populations: humans, mosquitoes, and bacteria. The total population of humans N_h is subdivided into seven classes which are susceptible S_h, vaccinated against typhoid fever V_t, infectious with malaria I_m, infectious with typhoid fever I_t, asymptomatic infected with typhoid fever A_t, infectious with malaria and asymptomatic with typhoid fever I_{mA_t}, and infectious with malaria and typhoid fever I_{mt}. The mosquito population is subdivided into two classes namely, susceptible S_v and infectious I_v. For mathematical tractability and convenience, and because the life-span of adult female mosquitoes that transmit the disease is generally short-lived, with only a small proportion living long enough (more than 10 days in tropical regions) to transmit malaria, we did not include the exposed class (see Figure 2). Let $B(t)$ denote the population of *Salmonella* bacteria at any time t. In contrast, the total populations of humans and mosquitoes are given by

$$N_h(t) = S_h(t) + V_t(t) + I_m(t) + A_t(t) + I_t(t) + I_{mA_t}(t) + I_{mt}(t),$$

$N_v(t) = S_v(t) + I_v(t)$ respectively.

In the human population, new arrivals at the constant rate Λ_h are only in the susceptible compartment, and all humans can die naturally at the rate μ_h. Infectious humans have an additional death due to the disease denoted by δ_1 for malaria, δ_2 for typhoid fever, and δ_3 for typhoid fever and malaria co-infections.

In the mosquito population, the new mosquitoes arrive in the susceptible class, and due to their short life span, all mosquitoes only die naturally at rate μ_v. Typhoid fever infected individuals I_t, A_t, I_{mA_t} and I_{mt} release bacteria into nature at the rate α_1, α_2, α_3 and α_4, respectively. These bacteria die at the constant rate μ_B. The rest of the transitions between the compartments is represented in Figures 1 and 2.

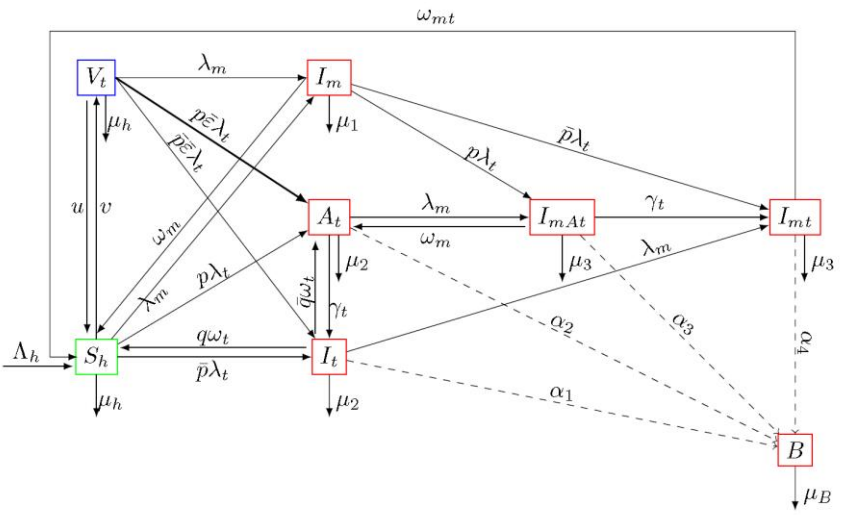

Figure 1
Compartmental diagram of the human population, where $\bar{p} = (1 - p)$, $\bar{q} = (1 - q)$, $\mu_1 = (\mu_h + \delta_m)$, $\mu_2 = (\mu_h + \delta_t)$, and $\mu_3 = (\mu_h + \delta_{mt})$.

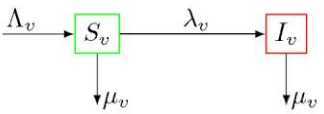

Figure 2
Compartmental diagram of the mosquito component of the model.

From the above model description and Figures 1 and 2, we derive the following nonlinear system of ordinary differential equations:

$$
\begin{aligned}
\dot{S}_h &= \Lambda_h + uV_t + \omega_m I_m + q\omega_t I_t + \omega_{mt} I_{mt} - (\lambda_m + \lambda_t + v + \mu_h)S_h,\\
\dot{V}_t &= vS_h - (\lambda_m + (1-\varepsilon)\lambda_t + u + \mu_h)V_t,\\
\dot{I}_m &= \lambda_m(S_h + V_t) - (\lambda_t + \omega_m + \mu_1)I_m,\\
\dot{A}_t &= p\lambda_t(S_h + V_t(1-\varepsilon)) + (1-q)\omega_t I_t + \omega_m I_{mAt} - (\lambda_m + \gamma_t + \mu_2)A_t,\\
\dot{I}_t &= (1-p)\lambda_t(S_h + V_t(1-\varepsilon)) + \gamma_t A_t - (\omega_t + \lambda_m + \mu_2)I_t,\\
\dot{I}_{mAt} &= \lambda_m A_t + p\lambda_t I_m - (\gamma_t + \omega_m + \mu_3)I_{mAt},\\
\dot{I}_{mt} &= (1-p)\lambda_t I_m + \lambda_m I_t + \gamma_t I_{mAt} - (\omega_{mt} + \mu_3)I_{mt},\\
\dot{B} &= (\alpha_1 I_t + \alpha_2 A_t + \alpha_3 I_{mAt} + \alpha_4 I_{mt}) - \mu_B B,\\
\dot{S}_v &= \Lambda_v - (\lambda_v + \mu_v)S_v,\\
\dot{I}_v &= \lambda_v S_v - \mu_v I_v,
\end{aligned}
\tag{1}
$$

subject to the initial conditions:

$$S_h(0) > 0, V_t(0) \geq 0, I_m(0) \geq 0, A_t(0) \geq 0, I_t(0) \geq 0, I_{mAt}(0) \geq 0,$$
$$I_{mt}(0) \geq 0, B(0) \geq 0, \; S_v(0) > 0, I_v(0) \geq 0. \quad (2)$$

The forces of infection for the bacteria, humans, and vector populations are defined as follows:

$$\lambda_t = \beta_t B, \lambda_m = \beta_m b \frac{I_v}{N_h},$$

and

$$\lambda_v = \beta_v b \frac{I_m + I_{mAt} + I_{mt}}{N_h},$$

respectively. The parameter b is the mosquito biting rate, while the parameters β_t, β_m, β_v represent respectively the infection rate of typhoid fever, the probability for a human to be malaria infected after a bite of an infected mosquito and the probability for a mosquito to be infected after a blood meal on a malaria infected human.

The model parameters, their description, values, and sources are presented in Table 1. Most values of the model parameters are from published literature; the rest are assumed for the purpose of illustration and summarized in Table 1 below. Note that, in Table 1, we assume that $\delta_{mt} = (\delta_m + \delta_t) = (1.8 \times 10^{-5} + 0.01)$. Note that inf. and asymp. in Table 1 stand respectively for infectious and asymptomatic.

Table 1
Model parameters' description, value and sources. The parameter values are normalized per day.

Parameter	Description	Value	Reference
humans			
v	Vaccination rate	0.5	Assumed
ε	Vaccine efficacy	[0.48, 0.956]	[10, 29]
δ_t	Death rate due to typhoid	0.01	[23]
δ_{mt}	Death rate due to co-infection of malaria and typhoid	$\delta_m + \delta_t$	Assumed
Λ_h	Recruitment rate of the host population	467	[25]
μ_h	Natural death rate of the host population	$\frac{1}{59\times365}$	[6, 11]
δ_m	Death rate due to malaria	1.8×10^{-5}	[6]
u	Vaccine waning rate	9.041×10^{-4}	[23]
b	Number of female mosquito bites per day	4.3×0.33	[9]
β_m	Malaria transmission probability per mosquito bite	[0.125, 0.5]	[14]
β_t	Infection rate of typhoid	1.37×10^{-9}	[25]
ω_m	Recovery rate of malaria infected individuals	0.0035	[9]
ω_t	Recovery rate of typhoid infected individuals	0.002	Assumed

ω_{mt}	Recovery rate of malaria and typhoid infectious individuals	0.0015	Assumed
γ	Typhoid progression rate from asymptomatic to infectious	0.009	Assumed
p	Proportion of newly Typhoid infected who become asymptomatic	[0,1]	Variable
Bacteria			
μ_B	Bacterial decay rate	0.0645	[25]
α_1	Bacteria excretion (infectious)	10	[25]
α_2	Bacteria excretion (asymptomatic)	1	[25]
α_3	Bacteria excretion (inf. malaria and asym. typhoid)	1	Assumed
α_4	Bacteria excretion (inf. malaria and inf. typhoid)	10	Assumed
Mosquitoes			
Λ_v	Recruitment rate of vectors	$\frac{10^4}{21}$	[11]
μ_v	Natural death rate of vectors	$\frac{1}{21}$	[6, 11]
β_v	Transmission probability in vectors from infected humans	0.48	[15]

3. Model analysis

Here, the Typhoid-fever only and malaria only sub-models are qualitatively analyzed.

3.1 *Typhoid only model*

From the model (1), the typhoid fever only model, which includes vaccination, is obtained by setting the following variables $E_m(t) = I_{mAt}(t) = I_{mt}(t) = 0$. Thus, the typhoid fever only model is given by the following system of nonlinear ordinary differential equations:

$$\begin{aligned}
\dot{S}_h &= \Lambda_h + uV_t + \omega_t I_t - (\lambda_t + v + \mu_h)S_h,\\
\dot{V}_t &= vS_h - ((1-\varepsilon)\lambda_t + u + \mu_h)V_t,\\
\dot{A}_t &= p\lambda_t(S_h + (1-\varepsilon)V_t) + \delta I_t - (\gamma_t + \mu_h + \delta_t)A_t,\\
\dot{I}_t &= (1-p)\lambda_t(S_h + (1-\varepsilon)V_t) + \gamma_t A_t - (\omega_t + \mu_h + \delta_t)I_t,\\
\dot{B} &= (\alpha_1 I_t + \alpha_2 A_t) - \mu_B B.
\end{aligned} \tag{3}$$

By adding the first four equations of the system (3), we obtain

$$\dot{N}_h = \Lambda_h - \mu_h N_h - \delta_t(A_t + I_t),$$

which implies that

$$\dot{N}_h \leq \Lambda_h - \mu_h N_h,$$

and some little algebraic manipulations yields

$$\limsup_{x\to\infty} N(t) \leq \frac{\Lambda_h}{\mu_h}. \tag{1}$$

Using (4), we obtain from the last equation of (3) that

$$\dot{B} \leq \frac{(\alpha_1+\alpha_2)\Lambda_h}{\mu_h} - \mu_B B.$$

Similarly as in equation (4),

$$\limsup_{x\to\infty} B(t) \leq \frac{(\alpha_1+\alpha_2)\Lambda_h}{\mu_h\mu_B}. \tag{5}$$

The above result implies that the solutions of system (3) are non-negative and bounded in the region

$$\Omega_t = \left\{(S_h, V_t, A_t, I_t, B) \in \mathbb{R}_+^5 : N_h(t) \leq \frac{\Lambda_h}{\mu_h}, B(t) \leq \frac{(\alpha_1+\alpha_2)\Lambda_h}{\mu_h\mu_B}\right\}.$$

That is, all solutions of the typhoid fever only model autonomous system (3) starting in Ω_t remain in Ω_t for all $t \geq 0$. This implies that Ω_t is positively invariant and all solutions starting on the boundary of Ω_t will be attracted to the interior of Ω_t. Thus, the model (3) is mathematically and epidemiologically well-posed, and it is sufficient to study its dynamics in Ω_t [21, 22].

3.1.1 Stability of the disease-free equilibrium

The disease-free equilibrium (DFE) of the typhoid fever only model system (3) is given by

$$\mathcal{E}_{tf}^0 = (S_h^0, V_t^0, A_t^0, I_t^0, B^0) = \left(\frac{\Lambda_h(u+\mu_h)}{\mu_h(u+v+\mu_h)}, \frac{\Lambda_h v}{\mu_h(u+v+\mu_h)}, 0,0,0\right). \tag{6}$$

The linear stability of $\mathcal{E}_{tf}^0$ is established using the next-generation operator method on system (3). Using the notations of [37], the matrices F and V for the new infection terms and the remaining transfer terms are given by

$$F = \begin{pmatrix} 0 & 0 & p\beta_t(S_h^0 + (1-\varepsilon)V_t^0) \\ 0 & 0 & (1-p)\beta_t(S_h^0 + (1-\varepsilon)V_t^0) \\ \alpha_2 & \alpha_1 & 0 \end{pmatrix},$$

and

$$V = \begin{pmatrix} (\gamma_t + \mu + \delta_t) & -(1-q)\omega_t & 0 \\ -\gamma_t & (\omega_t + \mu + \delta_t) & 0 \\ 0 & 0 & \mu_B \end{pmatrix}.$$

The control reproduction number of the typhoid fever only model (3) is the dominant eigenvalue of the next generation matrix FV^{-1} given by

$$\mathcal{R}_{c_{tf}} = \sqrt{\frac{(\alpha_1((1-p)g_1 + p\gamma_t) + \alpha_2(pg_2 + (1-p)(1-q)\omega_t))((1-\varepsilon)v + \mu_h + u)\Lambda_h\beta_t}{\mu_h\mu_B(\mu_h+u+v)K_1}}, \tag{7}$$

where

$$K_1 = (\mu_h + \delta_h)(\omega_t + \gamma_t + \mu_h + \delta_h) + q\omega_t\gamma_t, g_1 = \gamma_t + \mu_h + \delta_t,$$

and $g_2 = \omega_t + \mu_h + \delta_t$.

The basic reproduction number $R_{0_{tf}}$ of the typhoid only model (3) is the expected number of secondary infections from one primary typhoid infected

individual during its entire period of infectiousness in a fully naive or susceptible population [37]. This threshold $R_{0_{tf}}$ is obtained when no intervention is implemented. Thus, when $v = 0$ in $R_{c_{tf}}$,

$$R_{0_{tf}} = \sqrt{\frac{(\alpha_1((1-p)g_1+p\gamma_t)+\alpha_2(pg_2+(1-p)(1-q)\omega_t))(\mu_h+u)\Lambda_h\beta_t}{\mu_h\mu_B(\mu_h+u)K_1}}.$$

From Theorem 2 in [37], the DFE $\mathcal{E}^0_{tf}$ of the typhoid only model system 3 is locally asymptotically stable if $R_{c_{tf}} < 1$, and unstable otherwise.

3.1.2 Endemic equilibrium and bifurcation analysis

The endemic equilibrium $(S_h^*, V_t^*, A_t^*, I_t^*, B^{**})$ is the biologically feasible solution of the following system:

$$\begin{aligned}
&\Lambda_h + uV_t + \omega_t I_t^* - (\lambda_t + v + \mu_h)S_h^* = 0,\\
&vS_h^* - ((1-\varepsilon)\lambda_t + u + \mu_h)V_t^* = 0,\\
&p\lambda_t(S_h^* + (1-\varepsilon)V_t^*) + (1-q)\omega_t I_t^* - (\gamma_t + \mu_h + \delta_t)A_t^* = 0,\\
&(1-p)\lambda_t(S_h^* + (1-\varepsilon)V_t^*) + \gamma_t A_t^* - (\omega_t + \mu_h + \delta_t)I_t^* = 0,\\
&(\alpha_1 I_t^* + \alpha_2 A_t^*) - \mu_B B^* = 0.
\end{aligned} \tag{8}$$

Solving for each variable yields:

$$S_h^* = \frac{\Lambda_h K_1(B\beta_t(1-\varepsilon)+u+\mu_h)}{B\beta_t[((B\beta_t+v)(1-\varepsilon)+\mu+u)K_2+((2-\varepsilon)\mu_h+u)K_1]}, \tag{9}$$

where

$$K_2 = \mu_h(\gamma_h + \mu_h) + \delta_t(\delta_t + \gamma_h + 2\mu_h) + \omega_t(p(\mu_h + \delta_t) + q\gamma_h - \gamma_h),$$

$$V_t^* = \frac{vS_h^*}{(1-\varepsilon)\lambda_t+u+\mu_h}, \tag{10}$$

$$I_t^* = \frac{p\gamma_t\lambda_t(S_h^*+(1-\varepsilon)V_t^*)+(1-p)\lambda_t(\gamma_t+\mu_h+\delta_t)(S_h^*+(1-\varepsilon)V_t^*)}{(\gamma_t+\mu+\delta_t)(\omega_t+\mu_h+\delta_t)-(1-q)\omega_t\gamma_t}, \tag{11}$$

$$A_t^* = \frac{(1-p)(1-q)\lambda_t\omega_t(S_h^*+(1-\varepsilon)V_t^*)+p(\omega_t+\mu_h+\delta_t)(S_h^*+(1-\varepsilon)V_t^*)}{(\gamma_t+\mu_h+\delta_t)(\omega_t+\mu_h+\delta_t)-(1-q)\omega_t\gamma_t}. \tag{12}$$

By substituting the values above into the force of infection and after some algebraic manipulations and re-arrangement, we obtain the following quadratic equation, which is analyzed to investigate the possibility of multiple equilibria.

$$B(a_2B^2 + a_1B + a_0) = 0, \tag{13}$$

where

$$\begin{aligned}
a_0 &= \mu_h\mu_B(\mu_h + u + v)((\mu_h + \delta_t)(\omega_t + \gamma_t + \mu_h + \delta_t) + q\omega_t\gamma_t)(\mathcal{R}_{c_{tf}} - 1)\\
&= K_3(\mathcal{R}_{0_{tf}} - 1),\\
a_1 &= \Lambda_h(1-\varepsilon)\beta_t^2[\alpha_1(p\gamma_t + (1-p)(\gamma_t + \mu_h + \delta_t))]\\
&\quad -\mu_B\beta_t(\mu_h + u + v(1-\varepsilon))K_2,\\
a_2 &= -(1-\varepsilon)\mu_B\beta_t^2K_1.
\end{aligned}$$

For $\mathcal{R}_{c_{tf}} \neq 1$, the discriminant of this equation is given by

$$\Delta = a_1^2 + 4\mu_B\beta_t^2K_1K_3(1-\varepsilon)(\mathcal{R}_{0_{tf}}^2 - 1). \tag{14}$$

Therefore, $\Delta > 0 \Leftrightarrow \mathcal{R}_{c_{tf}}^2 > 1 - \frac{a_1^2}{4(1-\varepsilon)\mu_B\beta_t^2K_1K_3} = \mathcal{T}_{tf}$, and the following result summarizes the different cases.

Theorem 3.1:

1. *If* $\mathcal{R}_{c_{tf}} > 1$, *then, the model admits a unique endemic equilibrium.*
2. *If* $\mathcal{R}_{c_{tf}} = 1$, *and* $a_1 > 0$, *then, the model admits a unique endemic equilibrium.*
3. *If* $\mathcal{T}_{tf} < \mathcal{R}_{c_{tf}}^2 < 1$, *and* $a_1 > 0$, *then, the model admits two endemic equilibria.*
4. *Otherwise, the typhoid fever only model has no endemic equilibrium.*

The typhoid fever only model exhibits the phenomenon of backward bifurcation when condition 3 above is satisfied. This implies that having the basic reproduction number less than one will not be sufficient to eradicate typhoid fever in the population. Thus, to mitigate the spread of typhoid fever, additional efforts or stricter control measures and intervention strategies than initially expected are required. This will be investigated in Section 4.

3.2 *Malaria only model*

Because malaria is a mosquito-borne disease, transmission encompasses the interplay of critical features of host-vector-parasite interactions. By setting $V_t0, I_t(t) = 0, A_t(t) = 0, I_{mAt}(t) = 0, I_{mt}(t) = 0, B(t) = 0$, the malaria only model is given by

$$\begin{aligned}
\dot{S}_h &= \Lambda_h + \omega_m I_m - (\lambda_m + \mu_h)S_h,\\
\dot{I}_m &= \lambda_m S_h - (\omega_m + \mu_h + \delta_m)I_m,\\
\dot{S}_v &= \Lambda_v - (\lambda_v + \mu_v)S_v,\\
\dot{I}_v &= \lambda_v S_v - \mu_v I_v.
\end{aligned} \tag{15}$$

The feasible region of system (15) is given by

$$\Omega_m = \left\{(S_h, I_m, S_v, I_v) \in \mathbb{R}_+^4 : S_h(t) + I_m(t) \le \frac{\Lambda_h}{\mu_h}, S_v(t) + I_v(t) \le \frac{\Lambda_v}{\mu_v}\right\}.$$

Because all solutions the model system (15) starting in Ω_m will remain in Ω_m for all time $t \ge 0$, Ω_m is positively invariant and attracting.

3.2.1 Stability of the disease-free equilibrium

The DFE of the malaria only model 15 is given by

$$\mathcal{E}_m^0 = (S_h^0, I_h^0, S_v^0, I_v^0) = \left(\frac{\Lambda_h}{\mu_h}, 0, \frac{\Lambda_v}{\mu_v}, 0\right). \tag{16}$$

Similarly, as in the typhoid only model, using the next generation matrix method in [37], the basic reproductive number of the malaria only model is given by

$$\mathcal{R}_{0_m} = \sqrt{\frac{b^2\Lambda_v\mu_h\beta_m\beta_v}{\Lambda_h\mu_v^2(\omega_m+\mu_h+\delta_m)}}. \tag{17}$$

From Theorem 2 in [37], when $R_{0_m} < 1$, local asymptotic stability of the DFE of the malaria only model (15) follows, and the DFE is unstable otherwise.

3.2.2 Endemic equilibrium of the malaria only model

The endemic equilibrium of the model (15) is given by

$$S_h^* = \frac{\Lambda_h(\omega_m+\mu_h+\delta_m)}{(\delta_m+\mu_h)(\lambda_m+\mu_h)+\mu_h\omega_m}, I_m^* = \frac{\Lambda_h\lambda_m}{(\delta_m+\mu_h)(\lambda_m+\mu_h)+\mu_h\omega_m}, N_h^* = \frac{\Lambda_h-\delta_m I_m}{\mu_h},$$
$$I_v^* = \frac{\Lambda_v b\beta_v\lambda_m}{(b\beta_v\lambda_m+\delta_m\mu_v+\lambda_m\mu_v+\mu_h\mu_v+\mu_v\omega_m)\mu_v}. \tag{18}$$

By definition,

$$\lambda_m^* = \beta_m b\frac{I_v^*}{N_h^*}. \tag{19}$$

Substituting the values of I_v^* and N_h^* and after some rearrangements, we obtain the following quadratic equation:

$$\lambda_m^*[c_2\lambda_m^{2*} + c_1\lambda_m^* + c_0] = 0.$$

Thus, $\lambda_m^* = 0$, or

$$c_2\lambda_m^{2*} + c_1\lambda_m^* + c_0 = 0, \tag{20}$$

where

$$c_2 = -\Lambda_h\mu_v(b\beta_v + \mu_v) = -G_2,$$
$$c_1 = \Lambda_v^2 b^2\beta_m\beta_v(\mu_h + \delta_m) - \Lambda_h\mu_v(\omega_m + \mu_h + \delta_m)(b\beta_v + 2\mu_v),$$
$$c_0 = \Lambda_h\mu_v^2(\omega_m + \mu_h + \delta_m)^2(\mathcal{R}_{0_m}^2 - 1) = G_0(\mathcal{R}_{0_m}^2 - 1).$$

For $\mathcal{R}_{0_m} \neq 1$, the discriminant Δ_m of (20) is positive if and only if $\mathcal{R}_{0_m}^2 > \mathcal{T}_m = 1 - \frac{c_1^2}{4G_0G_2}$ Hence, we have established the following result.

Theorem 3.2

1. *If $\mathcal{R}_{0_m} > 1$, then, the malaria only model has one unique endemic equilibrium.*
2. *If $\mathcal{R}_{0_m} = 1$ and $c_1 > 0$, then the Malaria only model has one unique endemic equilibrium.*
3. *If $\mathcal{T}_m < \mathcal{R}_{0_m}^2 < 1$ and $c_1 > 0$, then, the malaria only model has two endemic equilibria.*
4. *Otherwise, the malaria only model has no endemic equilibrium.*

The malaria only model exhibits the phenomenon of backward bifurcation when condition 3 of the above Theorem is satisfied.

3.3 *Impact analysis of malaria-typhoid fever co-dynamics*

We determine the possible effect of malaria on typhoid fever and vice versa. To do this, we write $\mathcal{R}_{c_{tf}}$ in terms of $\mathcal{R}_{0_m}$. Using the expression of $\mathcal{R}_{0_m}$ yields

$$\Lambda_h = \frac{b^2\Lambda_v\mu_h\beta_m\beta_v}{\mu_v^2(\omega_m+mu_h+\delta_m)\mathcal{R}_{0_m}^2}. \tag{21}$$

Also, from the expression of $\mathcal{R}_{c_{tf}}$,

$$\Lambda_h = \frac{\mu_h\mu_B(\mu_h+u+v)K_1\mathcal{R}_{c_{tf}}^2}{(\alpha_1((1-p)g_1+p\gamma_t)+\alpha_2(pg_2+(1-p)(1-q)\omega_t))((1-\varepsilon)v+\mu_h+u)\beta_t}. \tag{22}$$

Equations (21) and (22) give the following relations between $\mathcal{R}_{c_{tf}}$ and $\mathcal{R}_{0_m}$:

$$\mathcal{R}_{c_{tf}} = \frac{1}{\mathcal{R}_{0_m}}\sqrt{\frac{b^2\Lambda_v\mu_h\beta_m\beta_v(\alpha_1((1-p)g_1+p\gamma_t)+\alpha_2(pg_2+(1-p)(1-q)\omega_t))((1-\varepsilon)v+\mu_h+u)\beta_t}{K_1\mu_v^2\mu_h\mu_B(\mu_h+u+v)(\omega_m+mu_h+\delta_m)}}. \tag{23}$$

Partially derivating $\mathcal{R}_{c_{tf}}$ with respect to $\mathcal{R}_{0_m}$ yields

$$\frac{\partial\mathcal{R}_{c_{tf}}}{\partial\mathcal{R}_{0_m}} = -\frac{1}{\mathcal{R}_{0_m}^2}\sqrt{\frac{b^2\Lambda_v\mu_h\beta_m\beta_v(\alpha_1((1-p)g_1+p\gamma_t)+\alpha_2(pg_2+(1-p)(1-q)\omega_t))((1-\varepsilon)v+\mu_h+u)\beta_t}{K_1\mu_v^2\mu_h\mu_B(\mu_h+u+v)(\omega_m+mu_h+\delta_m)}}. \tag{24}$$

Note that $\frac{\partial\mathcal{R}_{0_m}}{\partial\mathcal{R}_{c_{tf}}}$ is less than zero. The partial derivative of $\mathcal{R}_{c_{tf}}$ with respect to $\mathcal{R}_{0_m}$ and the partial derivative of $\mathcal{R}_{0_m}$ with respect to $\mathcal{R}_{c_{tf}}$ are all less than zero. So, the increase in the number of cases due to malaria could potentially lead to a decrease of the number of cases due to typhoid fever. Similarly, an increase in the number of cases of typhoid fever could potentially lead to a reduction in the number of cases due to malaria.

3.4 *Typhoid fever and malaria model*

The co-existence in the population of both malaria and typhoid fever are now considered. This means that a malaria infected individual can contract typhoid fever and become infected with both diseases, and vice versa.

3.4.1 Stability of the disease-free equilibrium of typhoid fever and malaria

The disease-free equilibrium of the malaria and typhoid fever model is given by

$$\begin{aligned}\mathcal{E}_{tm}^0 &= (S_h^0, V_t^0, I_m^0, A_t^0, I_{mAt}^0, I_{mt}^0, B^0, S_v^0, I_v^0)\\ &= \left(\frac{\Lambda_h(u+\mu_h)}{\mu_h(u+v+\mu_h)}, \frac{\Lambda_h v}{\mu_h(u+v+\mu_h)}, 0,0,0,0,0,0, \frac{\Lambda_v}{\mu_v}, 0\right).\end{aligned}$$

Since the disease threshold parameter for each sub-model (typhoid fever only and malaria only) using the next generation method in [37] has already been derived, the associated reproduction number for the full model (1) is given by

$$\mathcal{R}_{c_{tm}} = \max\{\mathcal{R}_{c_{tf}}, \mathcal{R}_{0_m}\}. \tag{25}$$

Again, from Theorem 2 in [37], the DFE of the typhoid fever and malaria co-dynamics model is locally asymptotically stable if the threshold parameter $\mathcal{R}_{c_{tm}} < 1$, and unstable otherwise.

The possible presence of two endemic equilibria respectively in the malaria only and Typhoid only sub-models above indicates the possibility of backward bifurcation in the full model (1) at $\mathcal{R}_{c_{tm}} = 1$ [22], if

$$max\{\mathcal{T}_{tf}, \mathcal{T}_m\} < min\left\{\mathcal{R}_{c_{tf}}, \mathcal{R}_{0_m}\right\} < \mathcal{R}_{c_{tm}} < 1 \text{ and } min\{a_1, c_1\} > 0.$$

4. Optimal control model

Optimal control for a given system deals with the problem of finding the best combination of control strategies. Thus, a control problem generally will include a function of state and control variables (a cost functional), while an optimal control is a set of differential equations describing the control variables that minimize the cost function. For more description and choice of quadratic cost functional below, see [17]. The following four steps will characterize the rest of this section: (i) description of the optimal control, (ii) proof of the existence of the optimal control problem, (iii) proof of the uniqueness of the optimal control and (iv) numerical simulations and graphical representations of the optimal control.

4.1 *Formulation of optimal control problem*

Three interventions, namely: reducing human contact with mosquitoes, vaccination and treatment against typhoid fever are proposed to mitigate the spread of malaria, typhoid fever and their potential co-infection. Thus, three time-varying controls $c_1(t)$, $c_2(t)$ and $c_3(t)$ are considered:

(a) $c_1(t)$ represents malaria prevention measures,

(b) $c_2(t)$ represents continuous vaccination against typhoid fever,

(c) $c_3(t)$ represents typhoid treatment.

These controls are incorporated into the model (1) as follows. First, multiply the force of infection λ_m and λ_v by $(1 - c_1(t))$. Second, replace the constant rate of vaccination v by $c_2(t)$ and the constant proportion q of infectious with typhoid fever that recovers by $c_3(t)$. Therefore, the optimal control model consists of the following non-autonomous nonlinear system of ordinary differential equations:

$$\begin{aligned}
\dot{S}_h &= \Lambda_h + uV_t + \omega_m I_m + c_3\omega_t I_t + \omega_{mt} I_{mt} - ((1-c_1)\lambda_m + \lambda_t + c_2 + \mu_h)S_h,\\
\dot{V}_t &= c_2 S_h - ((1-c_1)\lambda_m + (1-\varepsilon)\lambda_t + u + \mu_h)V_t,\\
\dot{I}_m &= (1-c_1)\lambda_m(S_h + V_t) - (\lambda_t + \mu_1)I_m,\\
\dot{A}_t &= p\lambda_t(S_h + V_t(1-\varepsilon)) + (1-c_3)\omega_t I_t + \omega_m I_{mAt} - (\lambda_m + \gamma + \mu_2)A_t,\\
\dot{I}_t &= (1-p)\lambda_t(S_h + V_t(1-\varepsilon)) + \gamma A_t - (\omega_t + (1-c_1)\lambda_m + \mu_2)I_t,\\
\dot{I}_{mAt} &= (1-c_1)\lambda_m A_t + p\lambda_t I_m - (\gamma + \omega_m\mu_3)I_{mAt},\\
\dot{I}_{mt} &= (1-p)\lambda_t I_m + (1-c_1)\lambda_m I_t + \gamma I_{mAt} - (\omega_{mt} + \mu_3)I_{mt},\\
\dot{B} &= (\alpha_1 I_t + \alpha_2 A_t + \alpha_3 I_{mAt} + \alpha_4 I_{mt}) - \mu_B B,
\end{aligned} \tag{26}$$

$$\dot{S}_v = \Lambda_v - ((1-c_1)\lambda_v + \mu_v)S_v,$$
$$\dot{I}_v = (1-c_1)\lambda_v s_v - \mu_v I_v.$$

The aim is to determine controls or combination of control strategies that if implemented will minimize the total number of infected individuals, that is, to find an optimal combination of the best control strategy while reducing the relative cost [17]. Thus, we wish to find the optimal values of $(c_1(t), c_2(t), c_3(t))$ that minimize the objective functional $J(c_1(t), c_2(t), c_3(t))$, where

$$J(c_1(t), c_2(t), c_3(t) = \int_0^T (A_1 I_m + A_2 A_t + A_3 I_t + A_4 I_{mAt} + A_5 I_{mt} + B_1 c_1^2(t) + B_2 c_2^2(t) + B_3 c_3^2(t).)dt \quad (27)$$

The functional in (27) takes into account the asymptomatic and infectious classes, and the cost of implementing each of the controls $c_1(t)$, $c_2(t)$, and $c_3(t)$. While the non-linearity of the controls allows the Hamiltonian to attain its minimum over the admissible control set, the choice of a quadratic control functional allows the positive balancing cost factors transfer the integral into monetary quantity over a finite time period [20, 17, 28]. The positive coefficients $A_i, 1 \leq i \leq 5$ and $B_i, 1 \leq i \leq 3$ are balancing weight parameters, while the controls $c_1(t)$, $c_2(t)$ and $c_3(t)$ are bounded, Lebesgue integrable functions [19, 20]. The main goal is to find an optimal control function $c_1^*(t)$, $c_2^*(t)$ and $c_3^*(t)$, such that

$$J(c_1^*, c_2^*, c_3^*) = min\{J(c_1, c_2, c_3) | c_1, c_2, c_3 \in \Gamma(T)\}, \quad (28)$$

with $\Gamma(T)$ the set of admissible controls defined as

$$\Gamma(T) = \{c_i | c_i(.) \text{ is Lebesgue mesurable on} [0, T], 0 \leq c_i(t) \leq 1, \forall t \in [0, T]\}.$$

4.2 *Existence and characterization of an optimal control*

To prove the existence of a potential optimal control for the model (26) and derive the optimality system, the following Theorem is applied.

Theorem 4.1: *Consider the objective functional J in (27), with $c_i \in \Gamma$ subject to the constraint state system (26). There exists $c_1^*, c_2^*, c_3^* \in \Gamma(T)$ such that $J(c_1^*, c_2^*, c_3^*) = min\{J(c_1, c_2, c_3) | c_1, c_2, c_3 \in \Gamma(T)\}$ subject to the control system {26} with initial conditions at $t = 0$.*

Proof: The state and control variables of the system (26) are positive, and the control set $\Gamma(T)$ is closed and convex. Therefore, the integrand of the objective functional J as expressed in the system (26) is a convex function of (c_1, c_2, c_3) on the control set $\Gamma(T)$. Since the state solutions are bounded, the Lipschitz property with respect to the state variables is satisfied. It can also be seen that there exist positive numbers ϖ_1 and ϖ_2 and a constant $\varpi_3 > 1$ such that

$$\varpi_1(|c_1|^2 + |c_2|^2 + |c_3|^2)^{\frac{\varpi_2}{2}} - \varpi_3 \geq J(c_1, c_2, c_3).$$

Boundness of the state variables follows and hence, the existence of an optimal control of the model (26).

4.3 *The uniqueness of optimal control*

Applying Pontryagin's maximum principle [30], necessary conditions that the three controls and corresponding state variables must satisfy are dereived. The Hamiltonian function for the system (26) where $\xi_i, 1 \leq i \leq 10$ are now the co-state variables or adjoints is defined as:

$$\begin{aligned}
\mathbb{H} = {} & A_1 I_m + A_2 A_t + A_3 I_t + A_4 I_{mAt} + A_5 I_{mt} + B_1 c_1^2(t) + B_2 c_2^2(t) + B_3 c_3^2(t) \\
& + \xi_1 \left(\Lambda_h + u V_t + \omega_m I_m + c_3 \omega_t I_t + \omega_{mt} I_{mt} - \left((1 - c_1) \frac{b \beta_m I_v}{N_h} + \beta_t B + c_2 + \mu_h \right) S_h \right) \\
& + \xi_2 \left(c_2 S_h - \left((1 - c_1) \frac{b \beta_m I_v}{N_h} + (1 - \varepsilon) \beta_t B + u + \mu_h \right) V_t \right) \\
& + \xi_3 \left((1 - c_1) \frac{b \beta_m I_v}{N_h} (S_h + V_t) - (\beta_t B + \mu_1) I_m \right) \\
& + \xi_4 \left(p \beta_t B (S_h + V_t (1 - \varepsilon)) + (1 - c_3) \omega_t I_t + \omega_m I_{mAt} - \left((1 - c_1) \frac{b \beta_m I_v}{N_h} + \gamma + \mu_2 \right) A_t \right) \\
& + \xi_5 \left((1 - p) \beta_t B (S_h + V_t (1 - \varepsilon)) + \gamma A_t - (\omega_t + (1 - c_1) \frac{b \beta_m I_v}{N_h} + \mu_2) I_t \right) \\
& + \xi_6 \left((1 - c_1) \frac{b \beta_m I_v}{N_h} A_t + p \beta_t B I_m - (\gamma + \omega_m + \mu_3) I_{mAt} \right) \\
& + \xi_7 \left((1 - p) \beta_t B I_m + (1 - c_1) \frac{b \beta_m I_v}{N_h} I_t + \gamma I_{mAt} - (\omega_{mt} + \mu_3) I_{mt} \right) \\
& + \xi_8 (\alpha_1 I_t + \alpha_2 A_t + \alpha_3 I_{mAt} + \alpha_4 I_{mt} - \mu_B B) \\
& + \xi_9 \left(\Lambda_v - \left(\mu_v + (1 - c_1) \frac{b \beta_v (I_m + I_{mAt} + I_{mt})}{N_h} \right) S_v \right) \\
& + \xi_{10} \left((1 - c_1) \frac{b \beta_v (I_m + I_{mAt} + I_{mt})}{N_h} S_v - \mu_v I_v \right).
\end{aligned} \tag{29}$$

The next Theorem presents the adjoint system and control characterization.

Theorem 4.2: *Given an optimal control c_1^*, c_2^* and c_3^* and corresponding state solutions $S_h, V_t, I_m, A_t, I_t, I_{mAt}, I_{mt}, B, S_v, I_v$ of the corresponding state system (1), there exists adjoint variables, $\xi_i, 1 \leq i \leq 10$, satisfying equation (32) given in Appendix. The controls c_1^*, c_2^* and c_3^* satisfy the following optimality*

$$\begin{aligned}
c_1^* &= max \left\{ 0, min \left(1, \frac{\lambda_m [S_h(\xi_3 - \xi_1) + V_t(\xi_3 - \xi_2) + A_t(\xi_6 - \xi_4) + I_t(\xi_7 - \xi_5)] + \lambda_v S_v (\xi_{10} - \xi_9)}{2 B_1} \right) \right\}, \\
c_2^* &= max \left\{ 0, min \left(1, \frac{S_h(\xi_1 - \xi_2)}{2 B_2} \right) \right\}, \\
c_3^* &= max \left\{ 0, min \left(1, \frac{\omega_t I_t (\xi_4 - \xi_1)}{2 B_3} \right) \right\}.
\end{aligned} \tag{30}$$

Proof: By applying Pontryagin maximum principle [30] yields the adjoint system below:

$$\begin{aligned}
\xi_1{}' &= -\frac{\partial \mathbb{H}}{\partial S} \quad \xi_2{}' = -\frac{\partial \mathbb{H}}{\partial V_t} \quad \xi_3{}' = -\frac{\partial \mathbb{H}}{\partial I_m}, \\
\xi_4{}' &= -\frac{\partial \mathbb{H}}{\partial A_t}, \quad \xi_5{}' = -\frac{\partial \mathbb{H}}{\partial I_t}, \quad \xi_6{}' = -\frac{\partial \mathbb{H}}{\partial I_{mAt}}, \\
\xi_7{}' &= -\frac{\partial \mathbb{H}}{\partial I_{mt}}, \quad \xi_8{}' = -\frac{\partial \mathbb{H}}{\partial B}, \quad \xi_9{}' = -\frac{\partial \mathbb{H}}{\partial S_v}, \quad \xi_{10}{}' = -\frac{\partial \mathbb{H}}{\partial I_v},
\end{aligned} \tag{31}$$

with zero final time conditions (transversality). The characterization of the optimal control given by (30) is obtained by solving the equations on the interior of the control set

$$\frac{\partial \mathbb{H}}{\partial c_1} = 0, \frac{\partial \mathbb{H}}{\partial c_2} = 0, \frac{\partial \mathbb{H}}{\partial c_3} = 0.$$

Using the bounds on the controls, we obtain the desired characterization.

5. Numerical simulations

Model simulations are generally used to graphically depict the long-term trajectory of complex nonlinear systems for which obtaining close form analytical solutions are a daunting task. The main objective herein is to evaluate the impact of optimal control on the spread of malaria and typhoid fever co-dynamics, as well as the effect the control of one of the diseases could have on another. Table 1 provides the model parameter values used for our numerical simulations. The fourth-order Runge-Kutta scheme is applied to the state equations (26). Then, the current iteration of the state equation are used to solve the adjoint equations (32) via a backward fourth-order Runge-Kutta scheme. For illustrative purposes, other parameter values are assumed as follows: the weight factor $A_1 = 5,\ A_2 = A_3 = A_4 = A_5 = 1, B_1 = 2.5,\ B_2 = 12$ and $B_3 = 2$, and the chosen initial conditions are $S_h(0) = 5000, V_t(0) = 0. I_m(0) = 50, A_t(0) = 10, I_{mAt}(0) = 40, I_{mt}(0) = 10,\ B(0) = 100, S_v(0) = 12000$ and $I_v(0) = 200$.

5.1 *Strategy 1: Typhoid fever prevention and treatment*

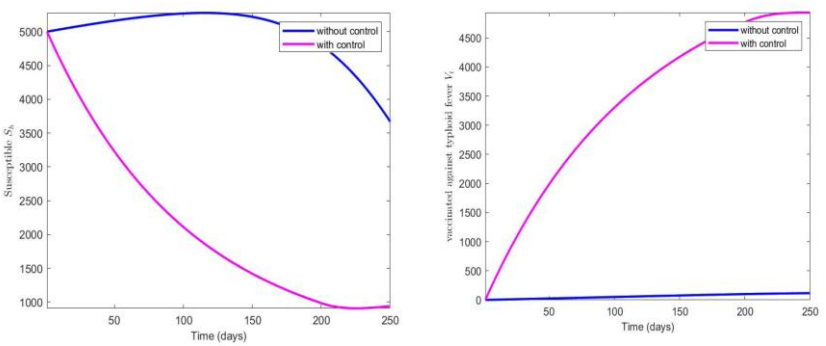

(a) Dynamics of susceptible individuals (b) Dynamics of vaccinated individuals

Figure 3
Time series evolution of susceptible and vaccinated against typhoid fever.

Figures 3a and 3b depict the time/dynamical evolution of the susceptible and vaccinated classes with and without controls (prevention (vaccination) of susceptibles against typhoid fever $c_2(t)$, and treatment of Typhoid $c_3(t)$). The simultaneous application of the two control interventions shows an increase in vaccinated individuals and a decrease in the number of susceptibles.

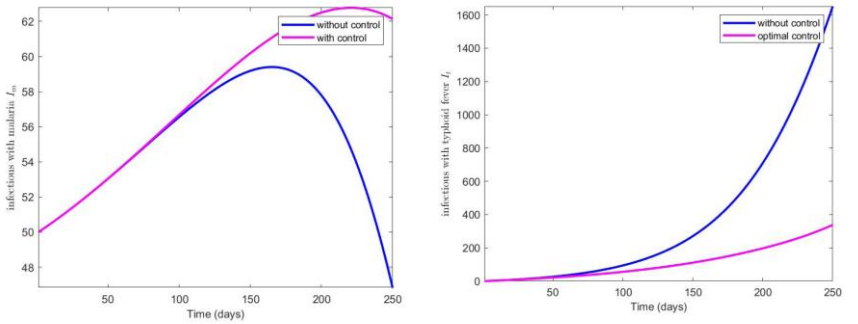

(a) Dynamics of infected with malaria I_m. (b) Dynamic of infected with typhoid I_t.

Figure 4
Time series evolution of malaria and typhoid fever infected individuals.

Figures 4a and 4b depict the dynamics of malaria infected and typhoid infected individuals. Simultaneous application of the two control interventions shows a positive population-level effect on the typhoid infected class resulting in a decrease in the number of these typhoid infected individuals. On the other hand, for the malaria infected class, there is no change in the infected during the ascending phase (0 to 100 days) when the control $c_3(t)$ is implemented. The change takes place at the level of the growth phase of the c_3 control. During this phase, there is a considerable increase in malaria infections.

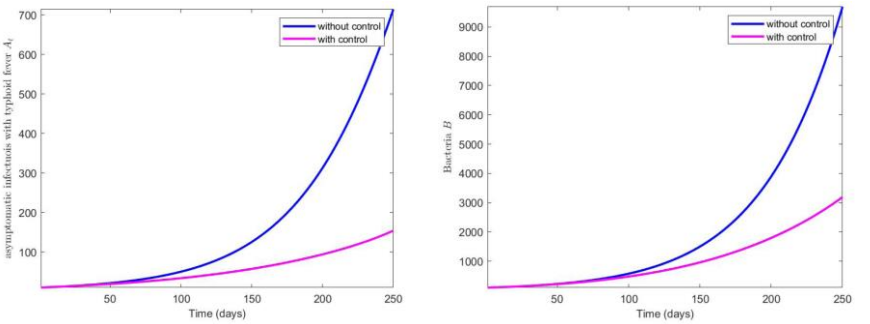

(a) Dynamic of typhoid asymptomatic class A_t (b) Dynamic of the bacteria $B(t)$.

Figure 5
Time series evolution of typhoid asymptomatic individuals and bacteria.

Figures 5a and 5b depicts typhoid asymptomatic class and bacteria dynamics. The application of this control strategy shows a positive population level effect on the asymptomatic typhoid class and the bacteria.

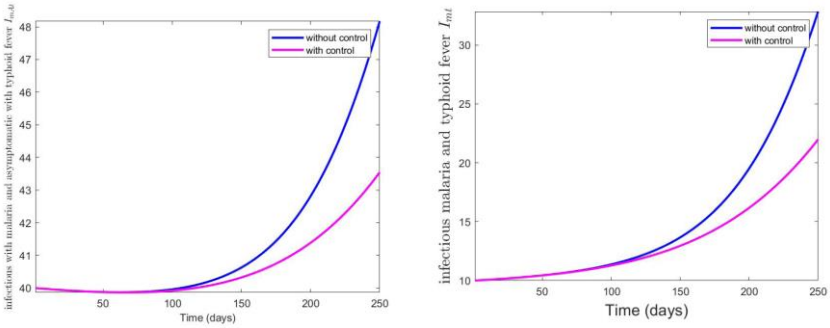

(a) Dynamics of malaria infected and typhoid asymptomatic class I_{mA_t}.

(b) Dynamic of I_{mt}

Figure 6

Time series showing simulations for malaria-typhoid asymptomatic and malaria-typhoid fever infectious individuals.

Figures 6a and 6b depict the dynamics of those infected with malaria, asymptomatic with typhoid fever, and those co-infected with malaria and typhoid fever. This control strategy makes it possible to reduce co-infections.

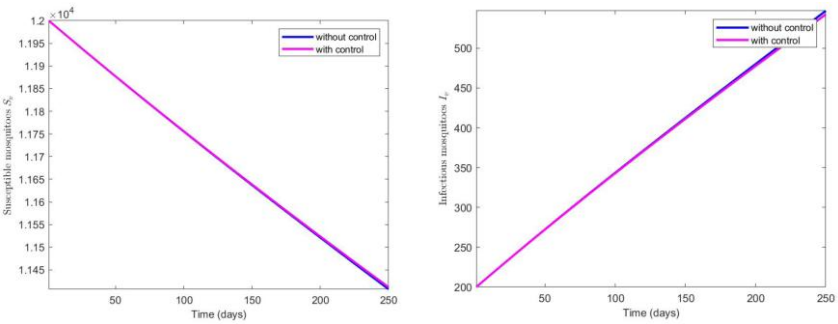

(a) Dynamic of susceptible vectors S_v.

(b) Dynamic of infected mosquitoes I_v

Figure 7

Time series evolution of susceptibles and infectious mosquitoes.

While typhoid therapeutic measures (prevention/vaccination $c_2(t)$ and treatment $c_3(t)$) do not directly impact the mosquito population, there is, however, a minimal impact on the latter as depicted in Figures 7a and 7b.

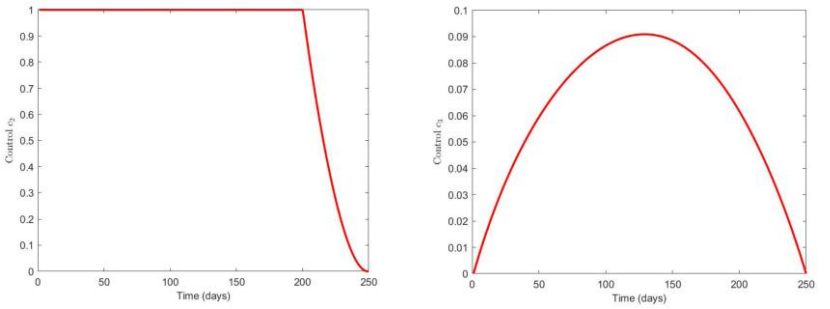

(a) Optimal control c_2 (b) Optimal control c_3

Figure 8
Control functions c_2 and c_3 where $c_1 = 0$

The control profiles of $c_2(t)$ and $c_3(t)$ are graphically depicted in Figures 8a and 8b. Vaccination starts at its upper bounds and is maintained until day 200 and then decreases, while $c_3(t)$ is a convex function that reaches its maximum at 150. In conclusion, this control strategy has a positive population-level effect on all compartments with the exception of those infected with malaria.

5.2 *Strategy 2: Malaria prevention and Typhoid fever treatment*

Strategy 2, which combines prevention against malaria and treatment against typhoid fever, seems to have a minimal population-level effect as the number of susceptibles with and without control is not significantly different, see Figure 9a. In the control model, the constant vaccination rate is replaced by the time-dependent control c_2, so for $c_2 = 0$, there is no vaccination in the control model, but we have constant vaccination in the model without control. Thus, Figure 9b is quite logical since the vaccination is not applied in control problem. Figures 10a and 10b show that this control strategy does minimally affect malaria infected and typhoid infected classes. This result is also valid for asymptomatic typhoid and bacteria (Figures 11a and 11b). The inefficiency of this strategy is more visible for co-infection, Figures 12a and 12b. The control profiles of malaria prevention $c_1(t)$ revealed that prevention is applied at the beginning of the intervention but only for a short time, and this supports the results in Figures 10a and 10b. The impact of the control on the vector is depicted in Figures 13a and 13b. For the treatment control, we have an increasing function which attains its maximum on day 200 and then decreases, see Figures 14a and 14b. The paradox with this strategy is that its effectiveness is only on typhoid infections and perhaps even on the co-infected class.

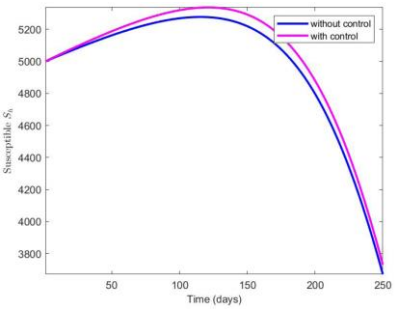

(a) Dynamic of susceptibles

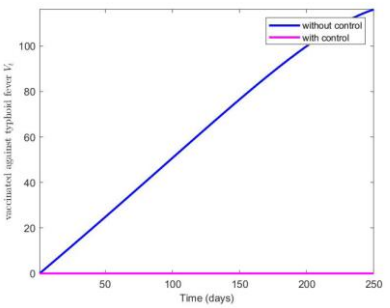

(b) Dynamic of vaccinated

Figure 9

Dynamics of susceptible and vaccinated classes against typhoid fever.

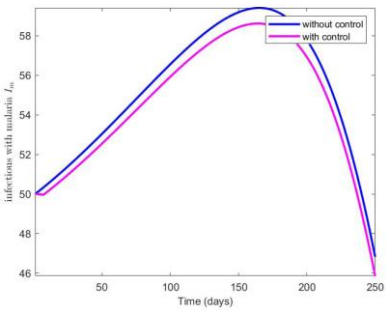

(a) Dynamic of I_m

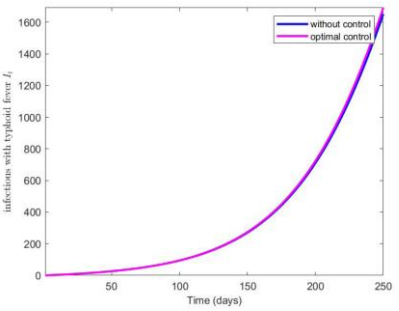

(b) Dynamic of I_t

Figure 10

Dynamics of malaria and typhoid infectious individuals.

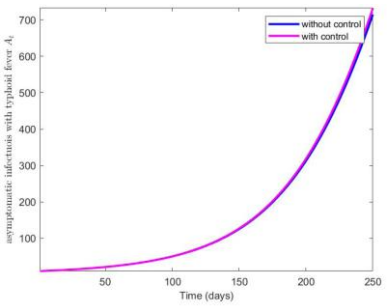

(a) Dynamics of typhoid asymptomatic individuals A_t.

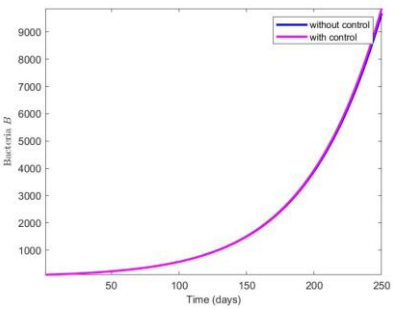

(b) Dynamic of bacteria $B(t)$

Figure 11

Time series of asymptomatic typhoid class and the bacteria.

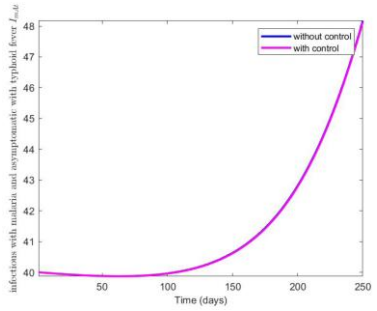

(a) Dynamic of infected with malaria and asymptomatic to typhoid I_{mA_t}

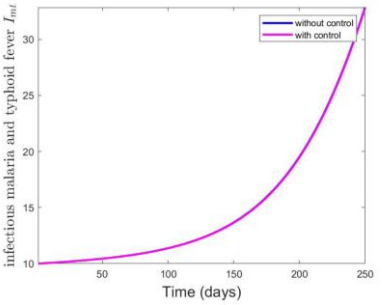

(b) Dynamic of infected with both malaria and typhoid fever I_{mt}

Figure 12

Time series evolution of individuals infected with malaria, asymptomatic with typhoid fever and infectious with both malaria and typhoid fever.

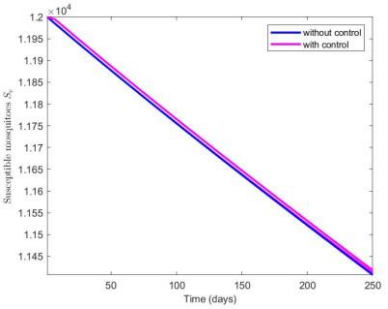

(a) Dynamic of susceptible vector S_v

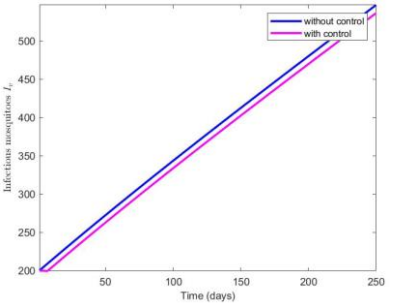

(b) Dynamic of infected mosquitoes I_v

Figure 13

Time series evolution of susceptible and infectious mosquitoes.

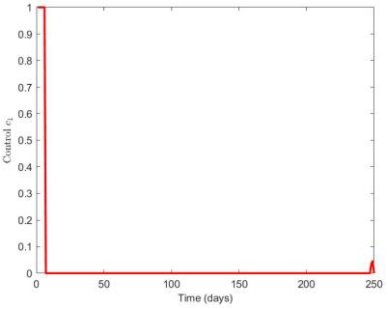

(a) Optimal control profile of malaria prevention c_1

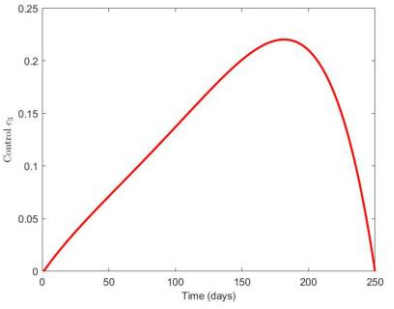

(b) Optimal control profile of typhoid treatment c_3

Figure 14

Control profiles of malaria prevention c_1 and typhoid treatment c_3 (no vaccination against typhoid fever $c_2 = 0$.)

5.3 *Strategy 3: Malaria prevention and typhoid fever prevention*

Strategy 3, which combines prevention and vaccination, is proving significant. In fact, Figures 15a and 15b show that the susceptible population is almost completely vaccinated. Prevention immediately affects those infected with malaria as seen in Figure 16a and typhoid Figure 16b. On the other hand, for co-dynamics, the effect is quite noticeable compared to strategy 2. This similar impact is carried over to the other classes as depicted in Figures 17a-19a. This strategy shows that infection with a single disease (malaria or typhoid) and co-infection can be reduced without typhoid treatment. However, treatment should continue to be administered to typhoid infected individuals. It is noted that the control for prevention is maintained at the maximum until the end of the intervention, while typhoid vaccination starts decreasing around day 190, Figures 20a, and 20b.

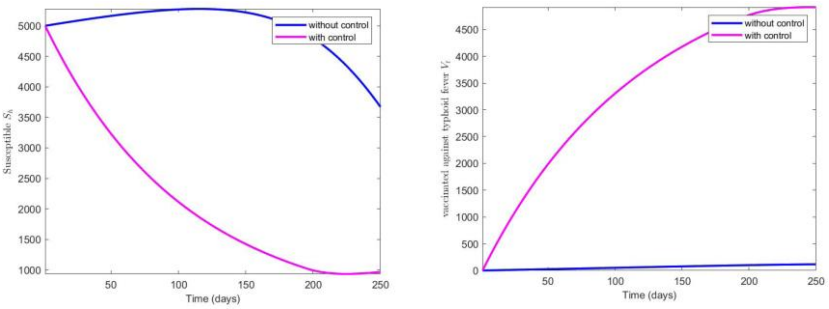

(a) Dynamic of susceptibles (b) Dynamic of vaccinated

Figure 15

Dynamics of susceptible and vaccinated individuals against typhoid fever.

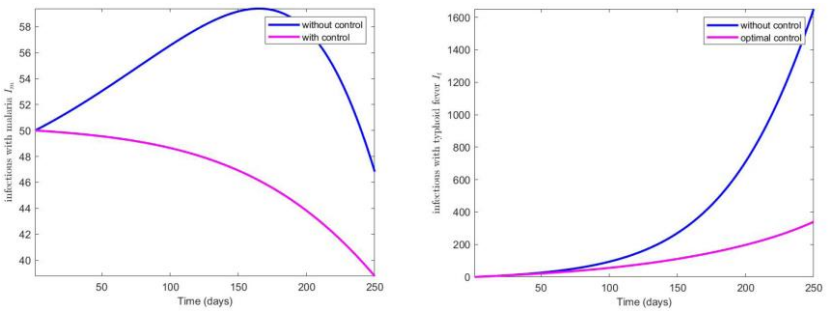

(a) Dynamic of I_m (b) Dynamic of I_t

Figure 16

Dynamics of malaria infectious and typhoid fever infectious individuals.

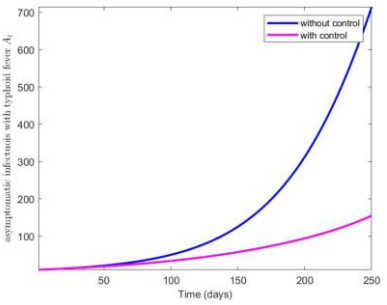

(a) Dynamic of malaria infectious individuals and asymptomatic with typhoid fever, A_t

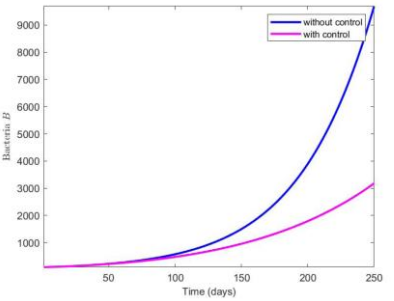

(b) Dynamic of bacteria

Figure 17

Dynamics of typhoid Fever asymptomatic infected individuals and bacteria.

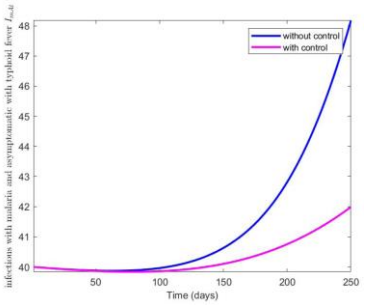

(a) Dynamic of infectious with malaria and asymptomatic with typhoid fever, I_{mA_t}

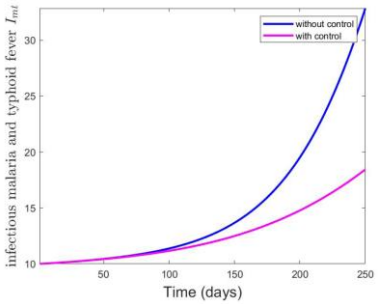

(b) Dynamic of co-infected with malaria and typhoid fever, I_{mt}

Figure 18

Dynamics of infectious with malaria and asymptomatic with typhoid fever and infectious with malaria and typhoid fever.

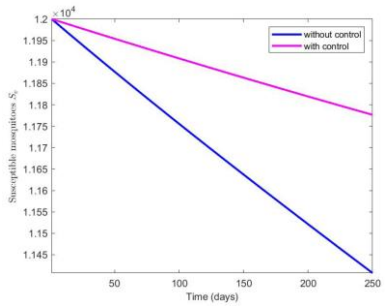

(a) Dynamic of susceptible mosquitoes, S_v

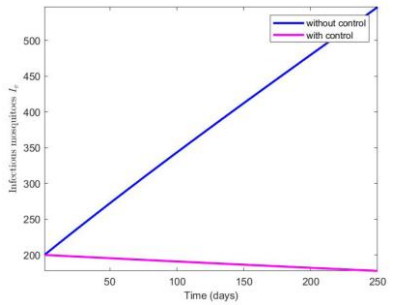

(b) Dynamic of infectious mosquitoes, I_v

Figure 19

Dynamics of susceptible and infectious mosquitoes.

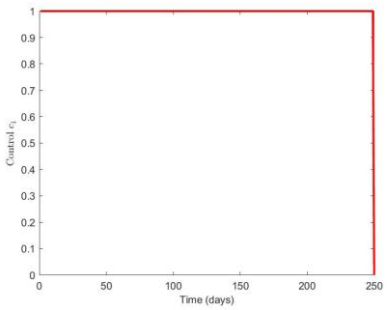

(a) Optimal control profile for malaria prevention, c_1

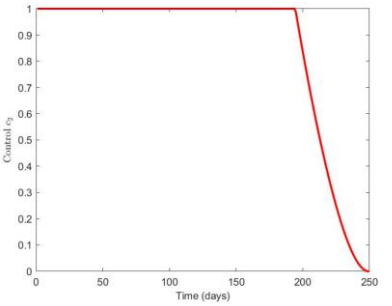

(b) Optimal control profile of vaccination against typhoid fever, c_2

Figure 20

Control functions c_1 and c_2 where treatment against typhoid fever $c_3 = 0$.

5.4 *Strategy 4: Malaria prevention, typhoid fever prevention and typhoid fever treatment*

As expected, concurrently implementing the three controls is more effective in mitigating the spread of both disease and their co-infection since towards the end of the implementation/simulation period, almost all susceptible individuals are vaccinated as depicted in Figures 21a and 21b. Also, infections, as well as the bacteria population, are reduced, Figures 22a-25b. These controls have an immediate population level effect on those infected with malaria, but one has to wait for 60 days to see the positive effect on those infected with typhoid. Co-dynamics are reduced from day 100. Malaria prevention is maintained at its maximum throughout the implementation of the control, Figure 26a, while vaccination against typhoid fever is maintained at a maximum until day 190 and then decreases, Figure 26b. Regarding typhoid treatment, the graph is a convex function (almost like a normal distribution) that attains its maximum on or around day 160, Figure 26c.

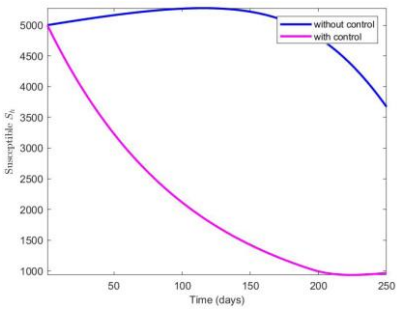

(a) Dynamic of susceptible

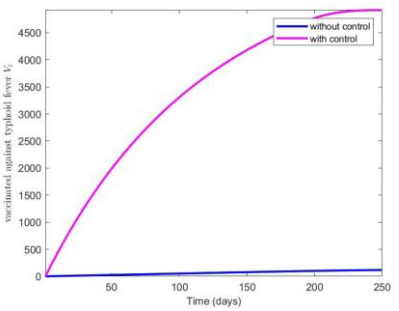

(b) Dynamic of vaccinated

Figure 21

Dynamics of susceptible and vaccinated against Typhoid Fever individuals.

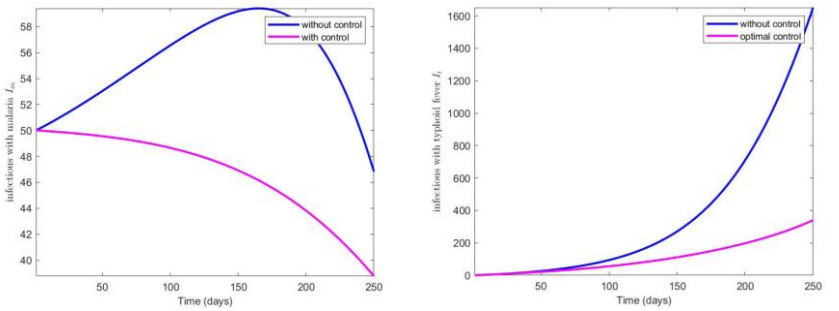

(a) Dynamic of I_m (b) Dynamic of I_t

Figure 22

Dynamic of malaria infectious and typhoid fever infectious individuals

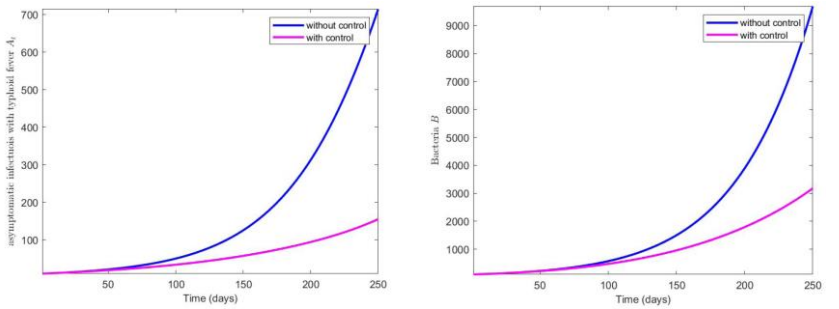

(a) Dynamic of A_t (b) Dynamic of Bacteria

Figure 23

Dynamics of typhoid fever asymptomatic infected individuals and bacteria.

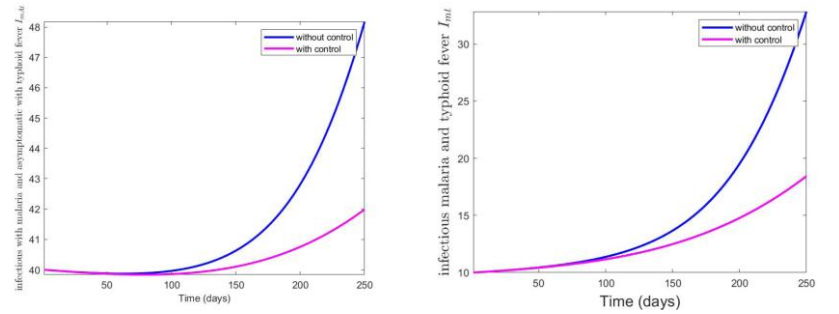

(a) Dynamic of I_{mA_t} (b) Dynamic of I_{mt}

Figure 24

Dynamic of infectious with malaria and asymptomatic with typhoid fever and infectious with malaria and typhoid fever.

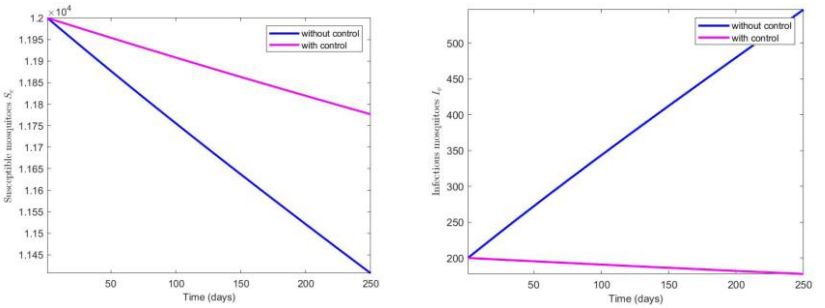

(a) Dynamic of S_v (b) Dynamic of I_v

Figure 25

Dynamics of susceptible and infectious mosquitoes.

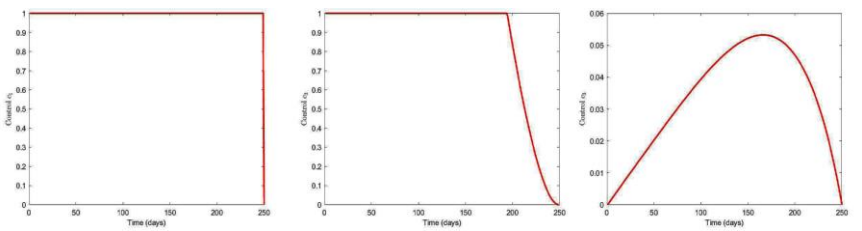

(a) Optimal control profile c_1 (b) Optimal control profile c_2 (c) Optimal control profile c_3

Figure 26

Control functions where $c_1 \neq 0$, $c_2 \neq 0$ and $c_3 \neq 0$.

6. Conclusion

Malaria is a vector-borne infectious disease that continues to cause morbidity and mortality in endemic areas worldwide, while typhoid fever is contracted by either drinking water or eating food contaminated with the *Salmonella* typhoid bacterium. Both diseases affects millions of individuals every year. While previous studies of the co-dynamics of these two diseases have not considered the interplay between typhoid symptomatic and asymptomatic individuals, these two classes are explicitly included in our proposed study by formulating a deterministic malaria and typhoid co-infection mathematical model that incorporates vaccination class (against typhoid), and the transitions between typhoid symptomatic and asymptomatic individuals. Using standard theory of dynamical systems, two sub-models and the full model are analyzed. The control or effective reproduction number for typhoid and the basic reproduction number for malaria are computed. Theoretical analysis of the model reveal that both the typhoid only and malaria only sub-models could exhibit the phenomenon of backward bifurcation, an epidemiological phenomenon where the disease persists in the population when the reproduction number is less than unity. That is, a stable DFE and a stable endemic equilibrium co-exist. In such a case, having the basic reproduction number less than unity is only necessary but not a sufficient

condition to mitigate the spread of the disease and additional control measures should be implemented in such a case to mitigate the spread of the infection [21, 22]. Investigation of the potential impact of malaria on typhoid and vice versa reveals not surprisingly that the increase in the number of cases due to malaria could potentially lead to a decrease of the number of cases due to typhoid fever, while an increase in the number of cases of typhoid fever could potentially lead to a reduction in the number of cases due to malaria.

Disease control is an important measure implemented to mitigate infectious diseases spread. To this end, the model is extended to include three intervention measures, namely: $c_1(t)$ for malaria prevention, $c_2(t)$ for typhoid vaccination, and $c_3(t)$ for typhoid treatment. Existence, characterization and uniqueness of an optimal control are provided. To gain more insights, using Matlab software, numerical simulations are carried out and results graphically depicted, which are summarized as follows:

(a) Reduction in the spread of typhoid greatly impacts reducing the number of malaria infectious individuals.

(b) The model analysis reveal as expected that the simultaneous implementation of the three control measures, namely prevention, treatment of infected individuals, and vaccination to reduce susceptibility to typhoid fever is the most effective optimal control strategy.

(c) Vaccination of typhoid plays a vital role in reducing the number of susceptible individuals who could acquire malaria-typhoid co-infection.

There are some limitations to the proposed model. Malaria treatment was not included as control measure in this study. With the development of a malaria vaccine for children below the age of five, extending the proposed model by including a two-group population to account for vaccination of children under five is important to align with the current knowledge about malaria epidemiology [34]. Notwithstanding these limitations, our proposed model could be used as a modeling framework to mitigate co-infection of malaria and typhoid fever. Finally, while our study is at a population level, an agent-based model is viable to account for individuals' intrinsic characteristics. Further studies at macro or micro-level with inputs from/collaboration with public health experts is important to ensure that the research question and anticipated results are appropriate and useful for policy making [26].

Acknowledgments

The authors thank their respective universities for the platform provided to carry out this work. SYT was supported by the DST/NRF SARChI Chair in Mathematical Models and Methods in Biosciences and Bioengineering at the University of Pretoria, South Africa, Grant No. N00317.

Disclosure statement

The authors declare they do not have any competing interests.

Funding

This work is not supported by any funding.

Author Contributions

Conceptualization: SYT and JMT; Formal analysis SYT ; Investigation: CWC, STY and JMT; Writing-original draft SYT, CWC, MLD Numerical simulations: SYT, MLD, Editing: SYT, MLD, CWC, HR and JMT. All authors agreed on the final version of the manuscript.

Appendix

The adjoint variables $\xi_i, 1 \leq i \leq 10$ satisfy the following system of equations

$$\begin{aligned}
\xi_1' &= \frac{b\beta_m(1-c_1)}{N_h^2}[S_h Iv(\xi_3-\xi_1)+V_t I_v(\xi_2-\xi_1)+A_t I_v(\xi_6-\xi_4)\\
&\quad +I_t I_v(\xi_7-\xi_5)]+\frac{b\beta_v(1-c_1)}{N_h^2}S_v(I_m+I_{mAt}+I_{mt})(\xi_{10}-\xi_9)\\
&\quad +\frac{b\beta_m(1-c_1)I_v}{N_h}(\xi_1-\xi_3)+\beta_t B(\xi_1-p\xi_4-(1-p)\xi_5)\\
&\quad +c_2(\xi_1-\xi_2)+\mu_h\xi_1\\
\xi_2' &= \frac{b\beta_m(1-c_1)}{N_h^2}[S_h Iv(\xi_3-\xi_1)+V_t I_v(\xi_3-\xi_2)+A_t I_v(\xi_6-\xi_4)\\
&\quad +I_t I_v(\xi_7-\xi_5)]\ +\frac{b\beta_v(1-c_1)}{N_h^2}S_v(I_m+I_{mAt}+I_{mt})(\xi_{10}-\xi_9)\\
&\quad +\frac{b\beta_m(1-c_1)I_v}{N_h}(\xi_2-\xi_3)\ +\beta_t(1-\varepsilon)B(\xi_2-p\xi_4-(1-p)\xi_5)\\
&\quad +u(\xi_2-\xi_3)+\mu_h\xi_2,\\
\xi_3' &= \frac{b\beta_m(1-c_1)}{N_h^2}[S_h Iv(\xi_3-\xi_1)+V_t I_v(\xi_3-\xi_2)+A_t I_v(\xi_6-\xi_4)\\
&\quad +I_t I_v(\xi_7-\xi_5)]\ +\frac{b\beta_v(1-c_1)}{N_h^2}S_v(I_m+I_{mAt}+I_{mt})(\xi_{10}-\xi_9)\\
&\quad +\frac{b\beta_v(1-c_1)S_v}{N_h}(\xi_9-\xi_{10})\ +\beta_t B(\xi_3-p\xi_6-(1-p)\xi_7)+\mu_1\xi_3-A_1,\\
\xi_4' &= \frac{b\beta_m(1-c_1)}{N_h^2}[S_h Iv(\xi_3-\xi_1)+V_t I_v(\xi_3-\xi_2)+A_t I_v(\xi_6-\xi_4)\\
&\quad +I_t I_v(\xi_7-\xi_5)]\ +\frac{b\beta_v(1-c_1)}{N_h^2}S_v(I_m+I_{mAt}+I_{mt})(\xi_{10}-\xi_9)\\
&\quad +\frac{b\beta_m(1-c_1)I_v}{N_h}(\xi_4-\xi_6)+\gamma(\xi_4-\xi_5)+\mu_2\xi_4-A_2,\\
\xi_5' &= \frac{b\beta_m(1-c_1)}{N_h^2}[S_h Iv(\xi_3-\xi_1)+V_t I_v(\xi_3-\xi_2)+A_t I_v(\xi_6-\xi_4)\\
&\quad +I_t I_v(\xi_7-\xi_5)]\ +\frac{b\beta_v(1-c_1)}{N_h^2}S_v(I_m+I_{mAt}+I_{mt})(\xi_{10}-\xi_9)\\
&\quad +\frac{b\beta_m(1-c_1)I_v}{N_h}(\xi_5-\xi_7)\ +\omega_t(\xi_5-(1-c_3)\xi_4-c_3\xi_1)-\alpha_1\xi_8\\
&\quad +\mu_2\xi_5-A_3,
\end{aligned}$$

$$\xi_6' = \frac{b\beta_m(1-c_1)}{N_h^2}[S_h Iv(\xi_3 - \xi_1) + V_t I_v(\xi_3 - \xi_2) + A_t I_v(\xi_6 - \xi_4) + I_t I_v(\xi_7 - \xi_5)] + \frac{b\beta_v(1-c_1)}{N_h^2} S_v(I_m + I_{mAt} + I_{mt})(\xi_{10} - \xi_9) + \frac{b\beta_v(1-c_1)S_v}{N_h}(\xi_9 - \xi_{10}) + \omega_m(\xi_6 - \xi_4) + \gamma(\xi_6 - \xi_7) - \alpha_2\xi_8 + \mu_3\xi_6 - A_4,$$

$$\xi_7' = \frac{b\beta_m(1-c_1)}{N_h^2}[S_h Iv(\xi_3 - \xi_1) + V_t I_v(\xi_3 - \xi_2) + A_t I_v(\xi_6 - \xi_4) + I_t I_v(\xi_7 - \xi_5)] + \frac{b\beta_v(1-c_1)}{N_h^2} S_v(I_m + I_{mAt} + I_{mt})(\xi_{10} - \xi_9) + \frac{b\beta_v(1-c_1)S_v}{N_h}(\xi_9 - \xi_{10}) + \omega_{mt}(\xi_7 - \xi_1) - \alpha_3\xi_8 + \mu_3\xi_7 - A_5,$$

$$\xi_8' = \beta_t S_h(\xi_1 - p\xi_4 - (1-p)\xi_5) + (1-p)\beta_t V_t(\xi_2 - p\xi_4 - (1-p)\xi_5) + \beta_t I_m(\xi_3 - p\xi_6 - (1-p)\xi_7) + \mu_B\xi_8,$$

$$\xi_9' = \frac{b\beta_v(1-c_1)}{N_h}(I_m + I_{mAt} + I_{mt})(\xi_9 - \xi_{10}) + \mu_v\xi_9,$$

References

[1] Mayo Clinic Staff, "Malaria – Symptoms and causes," Mayo Clinic, [Online]. Available: https://www.mayoclinic.org/diseases-conditions/malaria/symptoms-causes/syc-20351184. [Accessed: Mar. 5, 2024].

[2] World Health Organization, "Typhoid," WHO Fact Sheets, [Online]. Available: https://www.who.int/news-room/fact-sheets/detail/typhoid. [Accessed: Mar. 6, 2024].

[3] National Institute for Communicable Diseases, "Update on enteric fever in South Africa – 18 Feb (2022)," [Online]. Available: https://www.nicd.ac.za/update-on-enteric-fever-in-south-africa-18-feb-2022/. [Accessed: Mar. 7, 2024].

[4] Hamadou Abboubakar and Reinhard Racke, Mathematical Modelling and Optimal Control of Typhoid Fever (2019).

[5] Akeem Abdulfatai, Ismaila M. Ali, Blessing David, and Daniel J. Washachi, "Mathematical modelling of malaria and typhoid co-infection incorporating vector and loss of immunity," unpublished manuscript.

[6] Folashade B. Agusto, "Optimal isolation control strategies and cost-effectiveness analysis of a two-strain avian influenza model," *Biosystems*, vol. 113, no. 3, pp. 155–164 (2013).

[7] Ouma C. Akinyi, John Y. T. Mugisha, Andrew Manyonge, Charles Ouma, and Kennedy Maseno, "A model on the impact of treating typhoid with antimalarial: Dynamics of malaria concurrent and co-infection with typhoid," *International Journal of Mathematical Analysis*, vol. 9, no. 9–12, pp. 541–551 (2015).

[8] Adolf Ammah, Theresa Nkuo-Akenji, Roland Ndip, and J. E. Deas, "An update on concurrent malaria and typhoid fever in Cameroon," *Transactions of the Royal Society of Tropical Medicine and Hygiene*, vol. 93, no. 2, pp. 127–129 (1999).

[9] Roumen Anguelov, Yves Dumont, Jean M.-S. Lubuma, and Esau Mureithi, "Stability analysis and dynamics-preserving nonstandard finite difference schemes for a malaria model," *Mathematical Population Studies*, vol. 20, no. 2, pp. 101–122 (2013).

[10] Ehsan Anwar, Eliyahu Goldberg, Adam Fraser, Claudia J. Acosta, Mical Paul, and Leonard Leibovici, "Vaccines for preventing typhoid fever," *Cochrane Database of Systematic Reviews*, no. 1 (2014).

[11] Bruno Buonomo, "Analysis of a malaria model with mosquito host choice and bed-net control," *International Journal of Biomathematics*, vol. 8, no. 6, article 1550077 (2015).

[12] Ib Christian Bygbjerg, Claus Lanng, et al., "Septicaemia as a complication of falciparum malaria," *Transactions of the Royal Society of Tropical Medicine and Hygiene*, vol. 76, no. 5 (1982).

[13] Bill Bynum, "Typhomalarial fever," *The Lancet*, vol. 360, no. 9342, p. 1339 (2002).

[14] Jack Carr, Applications of Center Manifold Theory, New York, NY, USA: Springer-Verlag (1981).

[15] Nakul Chitnis, James M. Hyman, and James M. Cushing, "Determining important parameters in the spread of malaria through the sensitivity analysis of a mathematical model," *Bulletin of Mathematical Biology*, vol. 70, no. 5, pp. 1272–1296 (2008).

[16] C. W. Chukwu, M. L. Juga, Z. Chazuka, and J. Mushanyu, Mathematical analysis and sensitivity assessment of HIV/AIDS-listeriosis co-infection dynamics. *International Journal of Applied and Computational Mathematics*, 8(5), p.251 (2022).

[17] Mamadou L. Diagne, Folashade B. Agusto, Herieth Rwezaura, Jean M. Tchuenche, and Suzanne Lenhart, "Optimal control of an epidemic model with treatment in the presence of media coverage," *Scientific African*, vol. 24, article e02138 (2024).

[18] F. F. Herdicho, C. W. Chukwu, and H. Tasman, "An optimal control of malaria transmission model with mosquito seasonal factor," *Results in Physics*, vol. 25, article 104238 (2021).

[19] David Kirschner, Suzanne Lenhart, and Steve Serbin, "Optimal control of the chemotherapy of HIV," *Journal of Mathematical Biology,* vol. 35, no. 7, pp. 775–792 (1997).

[20] Suzanne Lenhart and John T. Workman, Optimal Control Applied to Biological Models. Boca Raton, FL, USA: Chapman and Hall/CRC (2007).

[21] Edmore Mtisi, Herieth Rwezaura, and Jean M. Tchuenche, "A mathematical analysis of malaria and tuberculosis codynamics," *Discrete and Continuous Dynamical Systems - Series B*, vol. 12, no. 4, pp. 827–847 (2009).

[22] Zindoga Mukandavire, Abba B. Gumel, Witness Garira, and Jean M. Tchuenche, "Mathematical analysis of a model for HIV-malaria coinfection," *Mathematical Biosciences and Engineering*, vol. 6, no. 2, pp. 333–362 (2009).

[23] Shelton Mushayabasa, Impact of vaccines on controlling typhoid fever in Kassana-Nankana district of Upper East Region of Ghana: Insight from a mathematical model (2011). [Unpublished or institutional report].

[24] Shelton Mushayabasa, Courage P. Bhunu, and N. A. Mhlanga, "Modeling the transmission dynamics of typhoid in malaria-endemic settings," *Applications and Applied Mathematics: An International Journal* (AAM), vol. 9, no. 1, article 9, pp. 49–65 (2014).

[25] Joseph M. Mutua, Feng-Bin Wang, and Nitin K. Vaidya, "Modeling malaria and typhoid fever co-infection dynamics," *Mathematical Biosciences,* vol. 264, pp. 128–144 (2015).

[26] Emmanuel Njeuhmeli, Melissa Schnure, Andrea Vazzano, Elizabeth Gold, Peter Stegman, Katharine Kripke, Michel Tchuenche, Lori Bollinger, Steven Forsythe, and Catherine Hankins, "Using mathematical modeling to inform health policy: A case study from voluntary medical male circumcision scale-up in Eastern and

Southern Africa and proposed framework for success," PLoS ONE, vol. 14, no. 3, article e0213605 (2019).

[27] Oluwadare M. Ogunmiloro, "Mathematical modeling of the co-infection dynamics of malaria-toxoplasmosis in the tropics," *Biometrical Letters*, vol. 56, no. 2, pp. 139–163 (2019).

[28] Bimala Pantha, Folashade Agusto, and Ibrahim Elmojtaba, "Optimal control applied to a visceral leishmaniasis model," (2020). [Unpublished or conference proceedings if no journal is specified].

[29] Virginia E. Pitzer, Catherine C. Bowles, Stephen Baker, Gagandeep Kang, Venugopal Balaji, Jeremy J. Farrar, and Bryan T. Grenfell, "Predicting the impact of vaccination on the transmission dynamics of typhoid in South Asia: A mathematical modeling study," *PLoS Neglected Tropical Diseases*, vol. 8, no. 1, article e2642 (2014).

[30] Lev S. Pontryagin, Vladimir G. Boltyanskii, Revaz V. Gamkrelidze, and Evgenii F. Mishchenko, The Mathematical Theory of Optimal Processes, vol. 4. New York, NY, USA: Interscience Publishers (1986).

[31] Israel Simon-Oke and Michael Akinbote, "Prevalence of malaria and typhoid co-infection in relation to haematological profile of university students in Akure, Nigeria," *Journal of Infectious Diseases and Epidemiology*, vol. 6, article 166 (2020).

[32] David C. Smith, "The rise and fall of typhomalarial fever: I. Origins," *Journal of the History of Medicine and Allied Sciences*, vol. 37, no. 2, pp. 182–220 (1982).

[33] H. Tasman, H., D. Aldila, P. A. Dumbela, M. Z. Ndii, Fatmawati, F. F. Herdicho, and C. W. Chukwu, "Assessing the impact of relapse, reinfection, and recrudescence on malaria eradication policy: A bifurcation and optimal control analysis," *Tropical Medicine and Infectious Disease*, vol. 7, no. 10, article 263 (2022).

[34] Stephane Y. Tchoumi, Chidozie W. Chukwu, Mamadou L. Diagne, Herieth Rwezaura, Mary L. Juga, and Jean M. Tchuenche, "Optimal control of a two-group malaria transmission model with vaccination," *Network Modeling Analysis in Health Informatics and Bioinformatics*, vol. 12, no. 1, article 7 (2022).

[35] Stephane Y. Tchoumi, Herieth Rwezaura, and Jean M. Tchuenche, "A mathematical model with numerical simulations for malaria transmission dynamics with differential susceptibility and partial immunity," *Healthcare Analytics*, vol. 3, article 100165 (2023).

[36] Getachew Teshome Tilahun and Haileyesus Tessema Alemneh, "Mathematical modeling and optimal control analysis of COVID-19 in Ethiopia," *Journal of Interdisciplinary Mathematics*, vol. 24, no. 8, pp. 2101–2120 (2021).

[37] Pauline Van den Driessche and James Watmough, "Reproduction numbers and sub-threshold endemic equilibria for compartmental models of disease transmission," *Mathematical Biosciences,* vol. 180, no. 1–2, pp. 29–48 (2002).

[38] World Health Organization, World Malaria Report 2021. [Online]. Available: https://www.who.int/publications/i/item/9789240040496. [Accessed: Feb. 5, 2024].

[39] Zemene Amare Workie and Poomani Raj Koya, "Mathematical modelling of the co-infection dynamics of typhoid fever with Plasmodium vivax and Plasmodium falciparum with treatment,".

Received March, 2024